TYPE Original Research
PUBLISHED 05 March 2024
DOI 10.3389/feart.2024.1355536

Check for updates

OPEN ACCESS

EDITED BY
Wen Chen,
Yunnan University, China

REVIEWED BY
Gang Zeng,
Nanjing University of Information Science and Technology, China
Peng Hu,
Chinese Academy of Sciences (CAS), China

*CORRESPONDENCE
Lin Liu,
liul@fio.org.cn

RECEIVED 14 December 2023
ACCEPTED 14 February 2024
PUBLISHED 05 March 2024

CITATION
Li Q, Liu L, Yang Y, Yang G, Duan Y and Zeng A (2024), The relationship between the Bay of Bengal summer monsoon retreat and early summer rainfall in East Asia.
Front. Earth Sci. 12:1355536.
doi: 10.3389/feart.2024.1355536

The relationship between the Bay of Bengal summer monsoon retreat and early summer rainfall in East Asia

Qiuchi Li[1,2], Lin Liu[1,2,3]*, Yang Yang[1,3], Guang Yang[1,3], Yongliang Duan[1,3] and Ai Zeng[1,4]

[1]First Institute of Oceanography, Ministry of Natural Resources and Laboratory for Regional Oceanography and Numerical Modeling, Pilot National Laboratory for Marine Science and Technology, Qingdao, China, [2]Southern Marine Science and Engineering Guangdong Laboratory (Zhuhai), Zhuhai, China, [3]Key Laboratory of Marine Science and Numerical Modeling, Ministry of Natural Resources, Qingdao, China, [4]Qingdao Innovation and Development Base, Harbin Engineering University, Qingdao, China

As the upstream region of the Asian summer monsoon, the Bay of Bengal summer monsoon (BOBSM) system has impacts on rainfall patterns in East Asia. In this study, we investigate the impact of the interannual variability of the BOBSM retreat on China precipitation in early summer (June) of the following year. When the BOBSM retreat occurs earlier in the previous year, we find enhanced rainfall in both the northeastern and eastern parts of China. Conversely, when the retreat of the BOBSM is delayed in the previous year, there is a tendency for decreased rainfall in most of northeastern and eastern China, while rainfall in the northern part of the Taiwan island region tends to increase. Statistical analysis demonstrates the co-variability between China's June precipitation anomalies and preceding wind anomalies in the eastern Bay of Bengal. The results indicate a strong relationship between the preceding BOBSM retreat and China precipitation anomalies in the following June. Furthermore, the analysis suggests that the BOBSM retreat is more of an independent signal rather than modulated by an Indian Ocean Dipole event.

KEYWORDS

Bay of Bengal summer monsoon, monsoon retreat, interannual variability, Indian Ocean Dipole, precipitation

1 Introduction

In summer, the onset of the monsoon brings abundant water vapor from the ocean inland, resulting in more frequent heavy precipitation. For instance, India is one of the countries most impacted by monsoonal rainfall, with the Indian summer monsoon (ISM) from June to September accounting for 70%–90% of the annual precipitation (Varikoden and Preethi, 2013; Hrudya et al., 2021). The rainfall in monsoon regions typically shows considerable interannual variability, which profoundly impacts agriculture in these areas and, consequently, the overall economy. Therefore, obtaining a better understanding of monsoon cycles can contribute not only to disaster prediction and the improvement of human development but also to our comprehension of the complex relationship between monsoons and precipitation.

Similar to India, the Asian summer monsoon also brings abundant precipitation to China every summer season. If we categorize the ISM and the Bay of Bengal summer monsoon (BOBSM) as parts of the ISM system, and classify the South China Sea summer monsoon (SCSSM) as part of the East Asian summer monsoon, it can be considered that the Asian summer monsoon system is roughly divided into two independent and interacting subsystems, both of which contribute to summer rainfall in different parts of China (Wang and Chen, 2012; Ding et al., 2016). The ISM plays a crucial role in the variation of precipitation in Southern China by transporting moisture from the Indian Ocean as part of the southwesterly branch, and the Bay of Bengal (BOB) serves as one of the main pathways for transporting tropical water vapor (Zhou and Yu, 2005; Zhang et al., 2021). Compared to the ISM, the impacts of the BOBSM and SCSSM on China's summer rainfall are more direct and significant after the onset of the summer monsoons, with the warm and humid airflows penetrating northward to mainland China. When the onset of the BOBSM occurs earlier than the climatological mean (late April), strong convective activity happens earlier over the BOB, which can cause rainfall in South China to be suppressed in May (Xing et al., 2016; Mao and Wu, 2007). Following the onset of the BOBSM, the onset of the SCSSM changes the precipitation pattern in South China from a notable drying trend to a wetting trend, which has been proven to strengthen its interdecadal relationship with the onset of the BOBSM (Zeng et al., 2021; Li et al., 2022). On the other hand, the retreat of the Asian summer monsoon has great impact on the precipitation in China, there is a significant positive correlation between the interannual variation in SCSSM retreat and September to October rainfall in Southern China (Hu et al., 2020). This may be associated with the retreat of the East Asian summer monsoon accompanied by the rainband moving southward (Chang, 2004; Chen et al., 2022). However, whether the retreat of the BOBSM is related to the subsequent rainfall in China has not received much attention. In this study, we attempt to reveal the relationship between the retreat of the BOBSM and the following June rainfall in China and provide some insights for rainfall prediction.

The rest of this paper is structured as follows. Section 2 provides an overview of the datasets and methodologies used in this study. Section 3 describes the relationship between the retreat of the BOBSM and China precipitation in the following June. *Discussion and conclusion* are presented in Section 4.

2 Data and methods

In the present study, observational and reanalysis datasets are used. Rainfall data come from version 2.3 of the monthly precipitation dataset of the Global Precipitation Climatology Project (GPCP, Adler et al., 2018), which is on a 2.5° × 2.5° grid from 1980 to 2022, and the National Oceanic and Atmospheric Administration's Precipitation Reconstruction over Land (PREC/L; Chen et al., 2002), which has a 0.5° × 0.5° horizontal resolution for the same period. The observational precipitation data from China, CN05.1 dataset is also used in this study (Wu and Gao, 2013), which has a 0.25° ×0.25° horizontal resolution interpolated from over 2,400 station observations. Three-dimensional variables, including zonal and meridional winds, are obtained from the European Centre for Medium-Range Weather Forecasts (ECMWF) and have a horizontal resolution of 0.25° × 0.25° (Hersbach et al., 2023), covering the same time period. The Indian Ocean Dipole Mode Index (DMI, Saji et al., 1999) is derived from the HadISST datasets provided by the Met Office Hadley Centre, which has a 1° × 1° spatial resolution and ranges from 1979 to 2022 (Rayner et al., 2003).

The BOBSM retreat index used the definition that is based on the areal mean zonal wind field at 850 hPa within the eastern BOB (90° ~ 100°E, 5° ~ 15°N, hereafter U850; Li et al., 2023). By defining the westward airflow as the positive direction, the definition of the retreat index is the first day after 1st October which also need satisfy the following criterions: (1) A shift in areal mean zonal wind from westly to easterly with a magnitude surpassing 1 m/s, (2) the magnitude of the average U850 over the subsequent 10 days (including the first day) must be less than −2 m/s, and (3) U850 should keep negative for at least 13 days within the following 15 days (including the first day).

Kinds of statistical methods including correlation, partial correlation, composite analysis and singular value decomposition (SVD) are used in this study. The formula of the correlation analysis is Eq. 1 as follows:

$$r_{x,y} = \frac{\sum_{i=1}^{n}\left(X_i - \overline{X}\right)\left(Y_i - \overline{Y}\right)}{\sqrt{\sum_{i=1}^{n}\left[\left(X_i - \overline{X}\right)\right]^2 \bullet \sum_{i=1}^{n}\left[\left(Y_i - \overline{Y}\right)\right]^2}} \tag{1}$$

where X_i and Y_i represents the retreat index and precipitation anomalies at each grid point respectively, $\overline{X}$ and $\overline{Y}$ represent the mean retreat index and climatological June precipitation respectively, n is the total year number. Partial correlation is employed to study the isolate impact of retreat of the BOBSM and the following June precipitation which removes the IOD signals. And formula of the partial correlation is Eq. 2 as follows:

$$r_{AB,C} = \frac{r_{AB} - r_{AC}r_{BC}}{\sqrt{1 - r_{AC}^2} \bullet \sqrt{1 - r_{BC}^2}} \tag{2}$$

Here, $r_{AB,C}$ means partial correlation coefficient between variables A and B after removing the influence of variable C, r_{ij} represents the linear correlation coefficient between two variables. In this study, variable A represents the BOBSM retreat index, variable B represents the June precipitation anomalies in the following year, and variable C represents the averaged DMI in previous SON season. The degrees of freedom for the t-test are n-3 (Ashok et al., 2007; Ding et al., 2016). On the other hand, the SVD analysis is utilized to extract the coupled modes between preceding wind anomalies in previous October and precipitation anomalies in following June (Bretherton et al., 1992; Zhang T. et al., 2022). The significance levels for correlation, partial correlation, and composite are tested by Student's t-test.

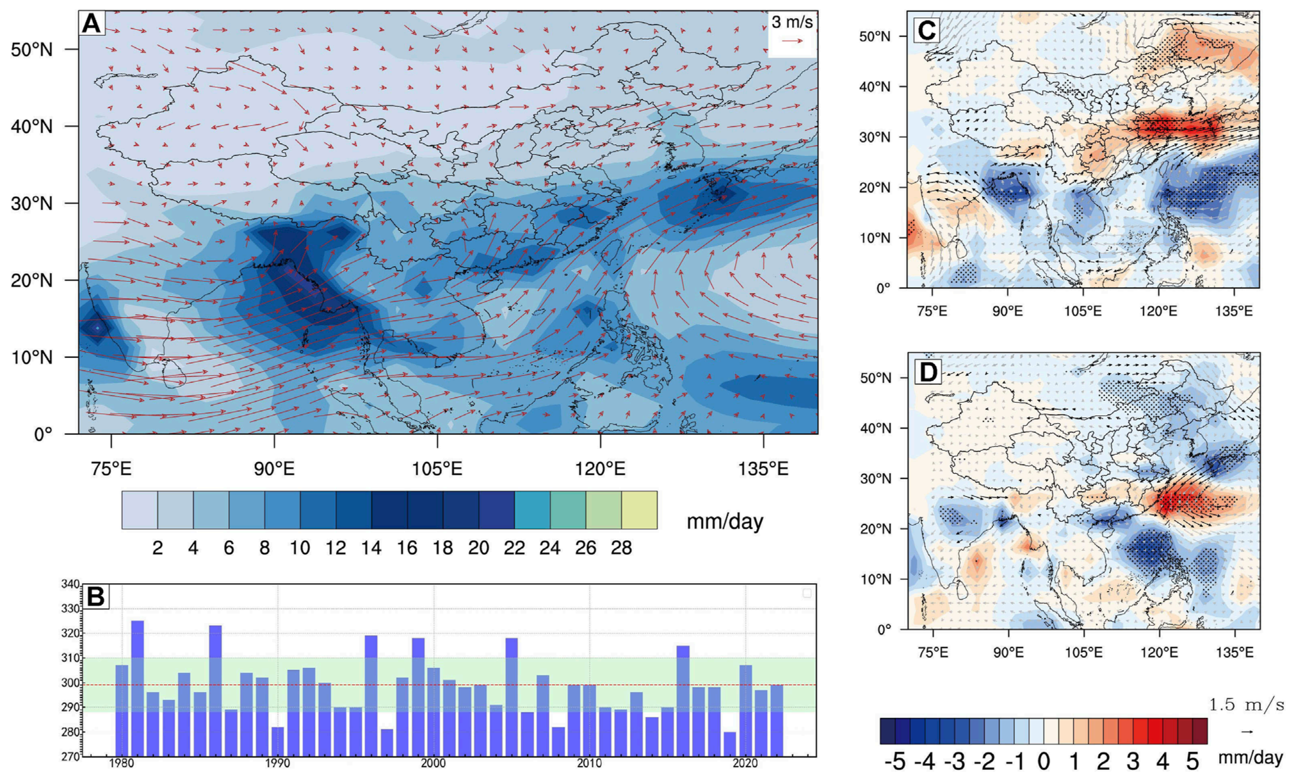

FIGURE 1
(A) Composite map for climatological mean wind fields at 850 hPa (vector, unit: m/s) and precipitation rate (shaded, unit: mm/day) for June during 1980 ~ 2022. **(B)** The BOBSM retreat index from 1980 to 2022 in Julian calendar and 7th October corresponds to 280 days. The red dot line represents the climatological mean retreat date and green shade line represents within one standard deviation (10 days). **(C)** Composite map for following June precipitation anomalies (shaded, unit: mm/day) and 850 hPa wind fields (vector, unit: m/s) after early retreat of BOBSM year, the scatter area passed the 95% significance level estimated by Student's t-test; **(D)** same as the **(C)** but under a late BOBSM retreat situation.

3 Results

3.1 Features of precipitation in June associated with BOBSM retreat

In June, climatological precipitation is mainly concentrated in the southern part of China. Figure 1A depicts the climatological wind pattern and precipitation rate for June during the period from 1980 to 2022, showing that southwesterly winds exceeding 3 m/s prevail over the Bay of Bengal (BOB) and flow eastward, reaching the South China Sea. Heavy rainfall occurs in the northwestern part of the Indo-China Peninsula, with precipitation rates exceeding 20 mm/day. The main precipitation belt is primarily concentrated in the Southern China, while precipitation in Northeast China is relatively weak due to the evolution of the summer monsoon.

At the interannual timescale, rainfall in China during June exhibits significant variability (Li et al., 2018; Zhao et al., 2018). As the first onset of the Asian summer monsoon, the BOBSM also shows interannual variation (Li et al., 2018), especially in its retreat phase. The BOBSM retreat index, shown in Julian calendar days, is listed in Figure 1B. It is noted that the retreat date of the BOBSM exhibits obvious interannual variation. The climatological retreat date of the BOBSM is October 26th (Julian day 299), as shown by the red dotted line. Assuming one standard deviation (10 days) as the criterion to judge the significant retreat year of the BOBSM, we define the selection criteria as follows: an early retreat event occurs when the Julian day number is smaller than 289. Conversely, a late retreat event occurs when the Julian day number is greater than 309. Using this criterion, significant early/late retreat events are identified as occurring in 1990, 1997, 2008, 2014, and 2019/1981, 1986, 1996, 2005, and 2016, respectively. The corresponding following years are 1991, 1998, 2009, 2015, and 2020/1982, 1987, 1997, 2000, 2006, and 2017.

To examine the rainfall anomaly distribution in the year following a significant BOBSM retreat, composite analysis is performed, as shown in Figures 1C, D. Figure 1C presents the composite map of precipitation anomalies in June following an early retreat of the BOBSM. Strong precipitation is observed in the northeastern and eastern parts of China, with abnormal southwesterly winds appearing at the lower level of 850 hPa in Eastern China. In contrast, Figure 1D shows the distribution of abnormal June precipitation following a late BOBSM retreat. There is a significant decrease in precipitation in Northeastern China, the Yangtze River valley in East China, and the northern part of the Beibu Gulf. Conversely, there is an increase in precipitation in

10.3389/feart.2024.1355536

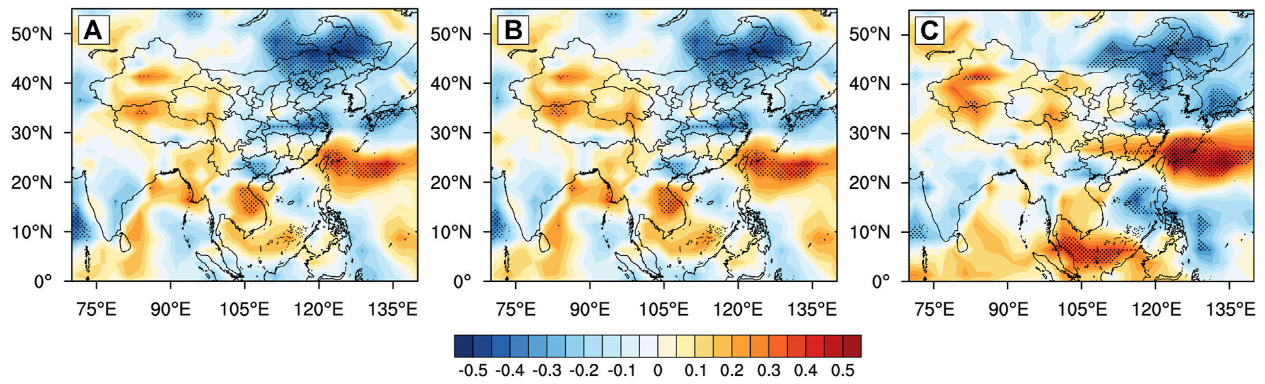

FIGURE 2
(A) Spatial distribution of the correlation between BOBSM retreat index (from 1980 to 2021) and the following June precipitation anomalies (from 1981 to 2022). **(B)** Same as the **(A)** but for detrend June precipitation anomalies. **(C)** Partial correlation between the retreat index and the June precipitation anomalies in the following year after removing IOD signals. The significance level is over 90% in the shaded area examined by Student's t-test.

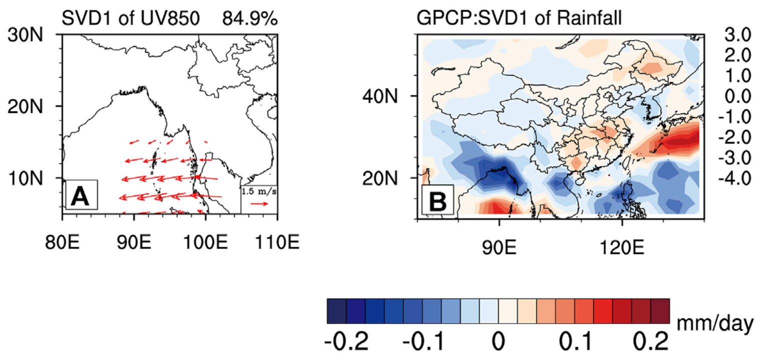

FIGURE 3
Spatial patterns of the first couple mode of **(A)** October winds anomalies (vectors) in eastern BOB at 850 hPa level, **(B)** rainfall anomalies in following June (contour, units: mm/day) and **(C)** the time series of wind filed and rainfall expansion coefficients respectively. The wind filed and rainfall are over periods of 1980–2021 and 1981–2022, respectively. The wind field was re-interpolated to a horizontal resolution of 2.5° ×2.5°.

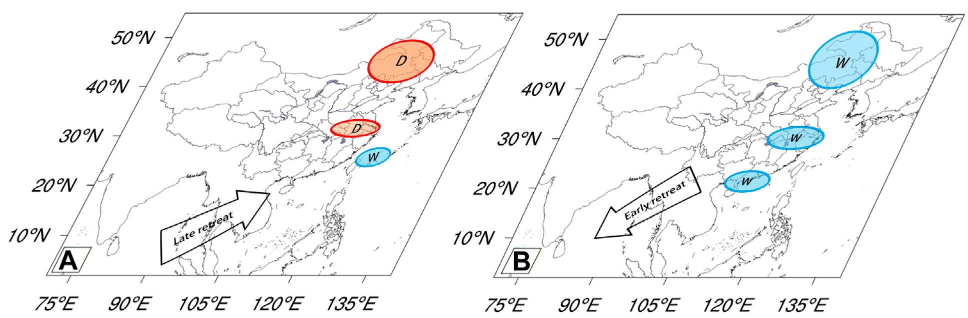

FIGURE 4
Conceptual map shows the area's following June precipitation effected by the retreat of the BOBSM. "D" means dry and "W" means wet. **(A)** Denotes the late retreat of the BOBSM. **(B)** Denotes the early retreat of the BOBSM.

and around Taiwan Island, accompanied by a cyclonic circulation anomaly at lower levels. Previous studies have also indicated that the aforementioned regions suffered significant drought or wet conditions in June following the alteration of the retreat time of the summer monsoon (Zhang et al., 2001; Wu et al., 2010; Guo et al., 2016; Zhang et al., 2017; Lee et al., 2023; Henny et al., 2023).

3.2 Relationship between BOBSM retreat and the following rainfall in June

In order to gain a deeper understanding of the relationship between the formal retreat of the BOBSM and the ensuing June precipitation in China, the Pearson correlation coefficient is calculated between the retreat index and the June precipitation anomalies in China. A negative correlation suggests that a delayed retreat of the BOBSM is associated with decreased rainfall, while an early retreat correlates with increased rainfall in the following June. Conversely, a positive correlation suggests that a delayed retreat is associated with increased rainfall, and an early retreat is associated with decreased rainfall in the following June. The correlation maps are shown in Figures 2A, B. To examine the role of IOD events, a partial correlation analysis is performed, and the results are presented in Figure 2C, and we will discuss in Section 4. Figure 2 demonstrates that the correlation between the retreat index and June precipitation in China is similar to the results of the composite maps (Figures 1C, D). The regions of Northeast and East China, as well as the northern part of the Beibu Gulf area, show a clear negative correlation, while a significant positive correlation is observed in the areas around Taiwan Island, consistent with the precipitation distribution revealed in the composite results. Additionally, similar results are confirmed by the analysis using the PREC/L and CN05.01 datasets (Supplementary Figure S1).

Considering the effect of abnormal circulation on the early or late retreat of the BOBSM in October, further analysis is conducted to explore the relationship between the abnormal wind field in the eastern BOB and the precipitation in the following June in China. By analyzing the covariance matrices of the wind field in the eastern BOB and the subsequent June precipitation, the SVD analysis is used to investigate the potential connection between June precipitation in China and the retreat date of the BOBSM. The results of the SVD, reveal that the first two modes explain 84.9% and 6.8% of the total variance, respectively. The cumulative variance explained by the first two modes is 91.8%, indicating that these modes (referred to as SVD1 and SVD2) effectively capture the dominant patterns of interaction between the retreat of the BOBSM and June rainfall. The first mode of SVD, as shown in Figure 3, accounts for 84.9% of the total variance in June precipitation anomalies over China. The time series corresponding to the first SVD mode of the wind field and June precipitation is illustrated in Figure 3C, with a correlation of 0.62 over the 42-year period. The wind field in the eastern BOB and precipitation exhibit consistent fluctuations during the study period (Figures 3A, B). And the SVD results indicate that when the corresponding time coefficient is positive, an abnormal northeasterly wind anomaly occurs in the eastern BOB, leading to an early retreat of the BOBSM. Concurrently, the associated precipitation mode is characterized by a tripole pattern over Northeastern China, Eastern China, and the northern part of the Beibu Gulf.

4 Discussion and conclusion

Previous studies have indicated that prior El Niño and Indian Ocean Dipole (IOD) events have a significant impact on summer precipitation in China, both El Niño and IOD can stimulate Western North Pacific anti-cyclonic circulation which form a favorable circulation pattern for June precipitation in China with different SST distributions. For instance, a strong positive IOD event with weak El Niño recorded in 2019 which contribute to extreme Yangtze River Valley flooding in 2020 by generating westward-propagating oceanic downwelling Rossby wave along the equator, result in a deepened thermocline favor for Indian Ocean warming from spring to summer in 2020, and the Indian Ocean warming forces an anomalous anticyclone in the lower troposphere over the Western North Pacific leading to heavy summer rains in Yangtze River Valley. (Li et al., 2007; Zhang et al., 2020; Zhou et al., 2021; Zhang Y. et al., 2022). Meanwhile, IOD events have a closely relationship with South Asian summer monsoon systems, a normal (late) SCSSM onset is associated with the previous positive (negative) IOD which also contribute to enhance (suppress) summer rainfall in China. (Yuan et al., 2008; Jiang et al., 2022). Furthermore, the interannual variation of the BOBSM retreat is also found to be modulated by IOD events, changes in the retreat of the BOBSM often coincide with the occurrence of IOD events, the early or delayed retreat of the BOBSM is related to a positive or negative IOD event, respectively (Li et al., 2023). Figures 2, 3 suggest a strong relationship between the anomalous wind field in the eastern BOB in the preceding October and the subsequent June rainfall in China. This raises the questions: How does the signal from the retreat of the BOBSM can persist 8 months to modulate the rainfall in China? Does the abnormal precipitation in June result primarily from IOD events, or from the relatively independent impact of the BOBSM retreat?

The spatial distribution pattern of the partial correlation (Figure 2C) is quite similar to that in Figure 2A. Northeast China and eastern part of Yangtze River Valley have a significant negative correlation with the BOBSM retreat index, which means heavy rains occur to these regions accompanying by the late retreat of the BOBSM in the previous year, and *vice versa* (Figures 1C, D, Figures 3c). Corresponding to obvious change in the retreat of the BOBSM, significant SST anomalies occur in the Indian Ocean and Pacific Ocean. SST may play an important role of modulating rainfall in the ensuing summer. SST warming in tropical Western North Pacific can modulate the retreat of the SCSSM tend to be late on one hand, and also resemble the developing phase of a La Niña which induce an anomalous cyclone over South China Sea at low-level via a Rossby wave-type atmospheric response, result in heavy rain in southern China from September to October (Hu et al., 2019; Hu et al., 2020; Chen et al., 2022; Hu et al., 2022). Similarly, late retreat of the BOBSM is accompanied by a La Niña and a negative IOD (Li et al., 2023). One possible dynamic mechanisms for explaining the linkage between the BOBSM retreat and summer rainfall in China is that when late retreat of BOBSM appeared with negative IOD, the late onset of the SCSSM next year will suppress the summer rainfall. However, this mechanism can only explain the precipitation in southern China, but not work on the abnormal precipitation in the Northeast China and the northern part of the Beibu Gulf occurring simultaneously. It suggests that the BOBSM retreat may be an independent factor impacting the subsequent June rainfall, rather than being solely influenced by IOD events, which potentially brings a tripole pattern of rainfall in China during the following June.

In this study, we explore the relationship between the retreat of the BOBSM and the subsequent June precipitation in China.

The statistical results indicate that the BOBSM retreat index is associated with the following June rainfall in China. An early retreat of the BOBSM can lead to increased precipitation in Northeastern China, Eastern China, and the northern part of the Beibu Gulf in the following June (Figure 4B). In contrast, a late retreat of the BOBSM can suppress precipitation in Northeastern and Eastern China but increase it in the Taiwan Island region (Figure 4A). This research reveals the relationship between the BOBSM retreat and the subsequent June rainfall, and the mechanism responsible for this correlation is still under investigation. Further work will be undertaken to elucidate the physical processes behind this correlation in the future.

Data availability statement

The datasets presented in this study can be found in online repositories. The names of the repository/repositories and accession number(s) can be found below: (1) https://cds.climate.copernicus.eu/cdsapp#!/dataset/reanalysis-era5-pressure-levels-monthly-means. (2) https://psl.noaa.gov/. (3) https://www.metoffice.gov.uk/hadobs/hadisst/. (4) https://ccrc.iap.ac.cn/resource.

Author contributions

QL: Data curation, Formal Analysis, Software, Visualization, Writing–original draft. LL: Conceptualization, Funding acquisition, Investigation, Methodology, Supervision, Writing–review and editing. YY: Data curation, Resources, Writing–review and editing. GY: Resources, Writing–review and editing. YD: Writing–review and editing. AZ: Data curation, Resources, Writing–review and editing.

Funding

The author(s) declare financial support was received for the research, authorship, and/or publication of this article. This work is supported by the Taishan Scholars Programs of Shandong Province (No. tsqn201909165), the Laoshan Laboratory (LSKJ202201703), the Global Change and Air-Sea Interaction Program (GASI-04-QYQH-03, GASI-01-WIND-STwin), and the Natural Science Foundation of China grants (41876028, 42349910).

Acknowledgments

We appreciated Dr. Yongjie Huang from IAP/CAS to provide China map database (https://github.com/huangynj/NCL-Chinamap.git). We also appreciated Dr. Tuantuan Zhang for providing NCL code of SVD analysis (Zhang T. et al., 2022).

Conflict of interest

The authors declare that the research was conducted in the absence of any commercial or financial relationships that could be construed as a potential conflict of interest.

Publisher's note

Supplementary material

The Supplementary Material for this article can be found online at: https://www.frontiersin.org/articles/10.3389/feart.2024.1355536/full#supplementary-material

References

Adler, R.-F., Sapiano, M., Huffman, G. J., Wang, J.-J., Gu, G., Bolvin, D., et al. (2018). The global precipitation Climatology Project (GPCP) monthly analysis (new version 2.3) and a review of 2017 global precipitation. *Atmosphere* 9 (4), 138. doi:10.3390/atmos9040138

Ashok, K., Behera, S. K., Rao, S. A., Weng, H., and Yamagata, T. (2007). El Niño Modoki and its possible teleconnection. *J. Geophys. Res.: Oceans* 112 (C11), C11007. doi:10.1029/2006jc003798

Bretherton, C. S., Smith, C., and Wallace, J. M. (1992). An intercomparison of methods for finding coupled patterns in climate data. *J. Clim.* 5 (6), 541–560. doi:10.1175/1520-0442(1992)005<0541:aiomff>2.0.co;2

Chang, C. (2004). East asian monsoon. *World Sci. Ser. Asia-Pacific Weather* 2, 572. doi:10.1142/5482

Chen, L., Chen, W., Hu, P., Chen, S., and An, X. (2022). Climatological characteristics of the East Asian summer monsoon retreat based on observational analysis. *Clim. Dyn.* 60, 3023–3037. doi:10.1007/s00382-022-06489-6

Chen, M., Xie, J.-E., Janowiak, P.-A., and Arkin, P. A. (2002). Global Land precipitation: a 50-yr monthly analysis based on gauge observations. *J. Hydrometeorol.* 3, 249–266. doi:10.1175/1525-7541(2002)003<0249:glpaym>2.0.co;2

Ding, S., Wen, Z., and Chen, W. (2016). Interdecadal change in the relationship between the South China Sea summer monsoon onset and two types of Pacific sea surface temperature anomaly. *Chin. J. Atmos. Sci.* 40 (2), 243–256. doi:10.3878/j.issn.1006-9895.1507.15102

Guo, D., Wang, L., Li, Z., Su, Y., Qin, H., and Huang, Y. (2016). Comparison between anomalies of summer rainfall in China in decaying years during super El Niño events of 2015/2016 and 1997/1998. *Trans. Atmos. Sci.* 39 (6), 835–844. doi:10.13878/j.cnki.dqkxxb.20160828010

Henny, L., Chris, D.-T., Huang, H.-H., and Lance, F.-B. (2023). Changes in extreme precipitation in Taiwan's Mei-yu season. *Q. J. R. Meteorol. Soc.* 149 (754), 1810–1832. doi:10.1002/qj.4483

Hersbach, H., Bell, B., Berrisford, P., Biavati, G., and Horányi, A. (2023). ERA5 monthly averaged data on single levels from 1940 to present. *Copernic. Clim. Change Serv. (C3S) Clim. Data Store (CDS).* doi:10.24381/cds.6860a573

Hrudya, P. H., Hamza, V., and Vishnu, R. (2021). A review on the Indian summer monsoon rainfall, variability and its association with ENSO and IOD. *Meteorol. Atmospheric Phys.* 133 (1), 1–14. doi:10.1007/s00703-020-00734-5

Hu, P., Chen, W., and Chen, S. (2019). Interdecadal change in the South China Sea summer monsoon withdrawal around the mid-2000s. *Clim. Dyn.* 52 (9–10), 6053–6064. doi:10.1007/s00382-018-4494-7

Hu, P., Chen, W., Chen, S., Liu, Y., Huang, R., and Dong, S. (2020). Relationship between the South China Sea summer monsoon withdrawal and September–October rainfall over southern China. *Clim. Dyn.* 54 (1–2), 713–726. doi:10.1007/s00382-019-05026-2

Hu, P., Chen, W., Wang, L., Chen, S., Liu, Y., and Chen, L. (2022). Revisiting the ENSO–monsoonal rainfall relationship: new insights based on an objective determination of the Asian summer monsoon duration. *Environ. Res. Lett.* 17 (10), 104050. doi:10.1088/1748-9326/ac97ad

Jiang, J., Liu, Y., Mao, J., Li, J., Zhao, S., and Yu, Y. (2022). Three types of positive Indian Ocean dipoles and their relationships with the South Asian summer monsoon. *J. Clim.* 35 (1), 405–424. doi:10.1175/jcli-d-21-0089.1

Lee, Y. C., Wenig, M. O., and Chan, K. L. (2023). Oceanic and atmospheric anomalies associated with extreme precipitation events in China 1983-2020. *Air Qual. Atmos. Health* 16 (5), 881–895. doi:10.1007/s11869-022-01295-9

Li, K., Liu, Y., Li, Z., Yang, Y., Feng, L., Khokiattiwong, S., et al. (2018a). Impacts of ENSO on the Bay of Bengal summer monsoon onset via modulating the intraseasonal oscillation. *Geophys. Res. Lett.* 45 (10), 5220–5228. doi:10.1029/2018gl078109

Li, Q., Liu, L., Duan, Y., Yang, G., Yang, Y., Luo, Y., et al. (2023). *Retreat of the Bay of Bengal summer monsoon*.

Li, W., Ren, H., Zuo, J., and Ren, H. (2018b). Early summer southern China rainfall variability and its oceanic drivers. *Clim. Dyn.* 50 (11–12), 4691–4705. doi:10.1007/s00382-017-3898-0

Li, Y., Deng, Y., Cheung, H.-N., Zhou, W., Yang, S., and Zhang, H. (2022). Amplifying subtropical hydrological transition over China in early summer tied to weakened mid-latitude synoptic disturbances. *NPJ Clim. Atmos. Sci.* 5, 40. doi:10.1038/s41612-022-00259-1

Li, Y., Wang, Y., and Wei, D. (2007). Effects of anomalous SST in tropical Indian Ocean and Pacific Ocean on next June rainfall over the Yangtze River basin and area south of the basin. *Acta Meteorol. Sin.* 2007 (3), 393–405. doi:10.11676/qxxb2007.037

Mao, J., and Wu, G. (2007). Interannual variability in the onset of the summer monsoon over the Eastern Bay of Bengal. *Meteorol. Atmospheric Phys.* 89 (3–4), 155–170. doi:10.1007/s00704-006-0265-1

Rayner, N. A., Parker, D. E., Horton, E. B., Folland, C. K., Alexander, L. V., Rowell, D. P., et al. (2003). Global analyses of sea surface temperature, sea ice, and night marine air temperature since the late nineteenth century. *J. Geophys. Res. Atmos.* 108, 4407. doi:10.1029/2002JD002670

Saji, N. H., Goswami, B. N., Vinayachandran, P. N., and Yamagata, T. (1999). A dipole mode in the tropical Indian Ocean. *Nature* 401 (6751), 360–363. doi:10.1038/43854

Varikoden, H., and Preethi, B. (2013). Wet and dry years of Indian summer monsoon and its relation with Indo-Pacific sea surface temperatures. *Int. J. Climatol.* 33 (7), 1761–1771. doi:10.1002/joc.3547

Wang, H., and Chen, H. (2012). Climate control for southeastern China moisture and precipitation: Indian or East Asian monsoon? *J. Geophys. Res.* 117, 017734. doi:10.1029/2012jd017734

Wu, J., and Gao, X. (2013). A gridded daily observation dataset over China region and comparison with the other datasets. *Chin. J. Geophys.* 56 (4), 1102–1111.

Wu, Y., Zhang, J., and Yan, Z. (2010). Analysis of an infrequent regional heavy rainfall weather process in Heilongjiang province in June of 2009. *Meteorol. Envir. Res.* 2010 (10), 11808–11809. doi:10.3969/j.issn.0517-6611.2010.22.055

Xing, N., Li, J., and Wang, L. (2016). Effect of the early and late onset of summer monsoon over the Bay of Bengal on Asian precipitation in May. *May. Clim. Dyn.* 47 (5–6), 1961–1970. doi:10.1007/s00382-015-2944-z

Yuan, Y., Yang, H., Zhou, W., and Li, C. (2008). Influences of the Indian Ocean dipole on the Asian summer monsoon in the following year. *Int. J. Climatol.* 28 (14), 1849–1859. doi:10.1002/joc.1678

Zeng, Z., Guo, Y., and Wen, Z. (2021). Interdecadal change in the relationship between the Bay of Bengal summer monsoon and South China sea summer monsoon onset. *Front. Earth Sci.* 8, 610982. doi:10.3389/feart.2020.610982

Zhang, R., Chu, Q., Zuo, Z., and Qi, Y. (2021). Summertime moisture sources and transportation pathways for China and associated atmospheric circulation patterns. *Front. Earth Sci.* 9, 756943. doi:10.3389/feart.2021.756943

Zhang, S., Tao, S., Zhang, Q., and Zhang, X. (2001). Meteorological and hydrological characteristics of severe flooding in China during the summer of 1998. *Q. J. Appl. Meteorol.* 12 (4), 442–457. doi:10.3969/j.issn.1001-7313.2001.04.007

Zhang, T., Jiang, X., Yang, S., Chen, J., and Li, Z. (2022). A predictable prospect of the South Asian summer monsoon. *Nat. Commun.* 13 (1), 7080. doi:10.1038/s41467-022-34881-7

Zhang, W., Zhou, X., Hsu, P.-C., and Liu, F. (2020). Diversity of East China summer rainfall change in post-el Niño summers. *Front. Earth Sci.* 8, 595548. doi:10.3389/feart.2020.595548

Zhang, Y., Zhang, L., Wang, S., and Feng, J. (2017). Drought events and its influence in summer of 2017 in China. *J. Arid. Meteorol.* doi:10.11755/j.issn.1006-7639(2017)-05-0899

Zhang, Y., Zhou, W., Wang, X., Chen, S., Chen, J., and Li, S. (2022). Indian Ocean Dipole and ENSO's mechanistic importance in modulating the ensuing-summer precipitation over Eastern China. *NPJ Clim. Atmos. Sci.* 5, 48. doi:10.1038/s41612-022-00271-5

Zhao, J., Zhou, J., Yang, L., Hou, W., and Feng, G. (2018). Inter-annual and inter-decadal variability of early- and late-summer precipitation over northeast China and their background circulation. *Int. J. Climatol.* 38 (6), 2880–2888. doi:10.1002/joc.5470

Zhou, T., and Yu, R. (2005). Atmospheric water vapor transport associated with typical anomalous summer rainfall patterns in China. *J. Geophys. Res.* 110, 5413. doi:10.1029/2004jd005413

Zhou, Z., Xie, S., and Zhang, R. (2021). Historic Yangtze flooding of 2020 tied to extreme Indian Ocean conditions. *Proc. Natl. Acad. Sci.* 118 (12), e2022255118. doi:10.1073/pnas.2022255118